JOURNAL OF CATALYSIS **171,** 293–304 (1997)
ARTICLE NO. CA971825

Effect of Steam Dealumination on H–Y Acidity and 2-Methylpentane Cracking Activity

M. A. Kuehne,* H. H. Kung,*,[1] and J. T. Miller†

*Ipatieff Laboratory and Department of Chemical Engineering, Northwestern University, Evanston, Illinois 60208-3120; and †Amoco Oil Company, P.O. Box 3011, Mail Station H-9, Naperville, Illinois 60566-7011

Received February 27, 1997; revised July 9, 1997; accepted July 11, 1997

The relationship between 2-methylpentane cracking activity and the acid properties of H–Y (acidic Y zeolite), H–USY (acidic ultrastable Y zeolite), steamed H–USY, and (H,NH_4)–USY ((H,NH_4)–ultrastable Y zeolite) was investigated. The acid strength distributions of these samples were determined by microcalorimetry of NH_3 adsorption, and the types of acid sites by FTIR spectroscopy. It was found that even for an H–Y sample of a high degree of crystallinity, its cracking activity per unit catalyst weight was 35 times lower than that of H–USY. With further steaming of H–USY, the cracking activity decreased, although the activity per strong Brønsted site remained essentially constant. Interestingly, although the strongly acidic Lewis acid sites were covered by NH_3 in (H,NH_4)–USY, the catalyst had the same activity as H–USY. Also, the heat of NH_3 adsorption on (H,NH_4)–USY did not exceed 130 kJ/mol. Thus, it was concluded that strong Lewis acid sites were not active for hydrocarbon cracking, and that 2-methylpentane cracking did not require Brønsted sites with a high heat of NH_3 adsorption. H–USY, with both Brønsted and Lewis sites, had a heterogeneous acid strength distribution, whereas zeolites containing only Brønsted sites had a homogeneous acid strength.

INTRODUCTION

The acidic form of ultrastable Y zeolite (H–USY), prepared by steam dealumination of Y zeolite, is a highly active hydrocarbon cracking catalyst. Brønsted acid sites are generated in USY by thermal decomposition of ammonium ions, which are exchanged into the zeolite, after the Y zeolite has undergone steam dealumination. Steam dealumination of (NH_4,Na)–Y zeolite at temperatures of 600–1100 K causes a partial removal of Al ions from the zeolite framework which are deposited in the zeolite pores, possibly as aluminum oxide or hydroxide cations (1–4). These Al species are referred to as extraframework (or nonframework) Al (Al_{NF}).

H–Y can also be prepared without nonframework Al by repeated NH_4^+ ion exchange of Na–Y to remove Na^+, followed by slow (dry) calcination at moderate temperatures to decompose the NH_4^+ ions. Because of its high Al content, H–Y displays poor thermal and hydrothermal stability, making it unsuitable for many commercial applications. In addition, despite more acid sites in H–Y than in H–USY, the catalytic activity of H–Y is much lower compared to H–USY (5). Thus, steam dealumination is important for development of high catalytic cracking activity and hydrothermal stability.

A number of explanations have been proposed for the higher activity of H–USY than of H–Y. The most prevalent proposal is that it is a result of increased Brønsted acid strength in H–USY. The increased acid strength is inferred from an increase in the ammonia desorption temperature by temperature programmed desorption (TPD) (6), an increased shift of the hydroxyl IR band frequency in response to hydrogen bonding with an adsorbed weak base (7), and microcalorimetry of adsorption of bases (8–10). The microcalorimetric and IR experiments also show the formation of strong Lewis acid sites in H–USY. However, they did not establish whether the strength of the Brønsted acid sites had increased.

Two reasons have been advanced to explain the higher activity and stronger acidity of H–USY (5). First, isolated framework Al (Al_F), i.e., those with no second nearest Al neighbors, are believed to be more acidic (11–14). Steam dealumination of the zeolite removes Al_F, which presumably results in more isolated Al_F. Second, it has been proposed (1) that nonframework Al species (Al_{NF}) next to Al_F withdraw electron density of the oxygen ions from the zeolite lattice. The Al_{NF} cations may be located in the sodalite cages (5) or may be Lewis acid sites near the Brønsted site (1, 15). This latter proposal is consistent with the observations that a small concentration of sodium (3, 15, 16), potassium (16), or ammonium (17) ions can destroy the activity of H–USY for cracking of C_4–C_7 hydrocarbons, presumably by poisoning the strongest acid sites (18).

Lewis acid sites also could enhance cracking activity, because H–USY has strong Lewis acid sites not present in H–Y, and a number of reports have proposed a catalytic role

[1] To whom correspondence should be addressed.

0021-9517/97 $25.00

of Lewis sites in zeolites. For example, it was suggested that Lewis sites might initiate cracking by abstracting H_2, CH_4 (19), or hydride ion (20) from paraffin molecules. Similarly, Lewis sites were proposed to initiate cracking of alkylbenzenes by abstracting a hydrogen ion or radical (21). Another study concluded that Lewis sites play no role in initiation of hydrocarbon cracking, but they do accelerate processes which produce aromatics and coke (22). More recently, it was shown that isomerization activity depends on the product of the Brønsted and Lewis acid site concentrations (23), suggesting a synergistic mechanism involving both types of sites. However, Lewis sites alone had no significant activity for *n*-hexane cracking in H−USY, after the strong Brønsted sites were poisoned selectively (24).

Most models for the high activity of H−USY involve a catalytic role for Al_{NF} species, because considerable evidence suggests that these species are required for high cracking activity in Y zeolites. In particular, zeolites with Al_{NF} have much higher cracking activity than those without Al_{NF}, but with similar Al_F content (4, 25, 26). Extraction of Al_{NF} decreases gas oil cracking activity (27), but recently it was reported that Al_{NF} extraction increases 2-methylpentane cracking activity, possibly because the Al_{NF} was blocking access to active sites (28). Various roles for Al_{NF} in catalytic cracking have been proposed. Al_{NF} might contain Lewis acid sites (29, 30), or it might enhance the acidity of Brønsted sites (1, 5, 15). Alternatively, Al_{NF} may form amorphous silica–alumina within the pores which is more catalytically active than the zeolite acid sites (31), although amorphous silica alumina is generally less active (32).

In this study, the acidity and 2-methylpentane cracking activity of H−Y, H−USY, and (H,NH_4)−USY were directly compared. Acid strength distributions were determined by NH_3 adsorption microcalorimetry, and FTIR of NH_3 adsorption was employed to distinguish between Lewis and Brønsted acidity. The acidic properties of the catalysts were related to their cracking activity, thus demonstrating both the applicability and limitations of calorimetry to the evaluation of acid catalysts.

EXPERIMENTAL

Catalyst Preparation

Na−Y (LZ-Y52) was a commercial zeolite obtained from UOP. NH_4−Y was prepared by ion exchange of Na−Y 10 times in a 10% NH_4NO_3 solution at 353 K, 100 g zeolite/liter. H−Y was prepared from NH_4−Y by heating at a rate of 2 K/min to 573 K and then maintaining at 573 K for 16 h in flowing air or dried N_2 (0.5 g; 60 cm^3/min). Because H−Y after exposure to air is unstable to heating, it was prepared *in situ* for each experiment. H−USY(26) was prepared from a commercial NH_4−USY (UOP, LZ-Y84) by calcining in air at 723 K for 16 h. Two steamed H−USY were prepared. H−USY(17) was prepared by steaming H−USY(26) in 101 KPa H_2O at 808 K for 1 h, and H−USY(8) at 973 K for 3 h. The catalysts and treatments are listed in Table 1. The zeolites are designated by their Al_F/unit cell in parentheses. A portion of sample H−USY(26) was converted back to the ammonium form by exchanging three times in NH_4NO_3 solutions of increasing concentration (0.5, 1, and 2 *M*) at 333 K for 8–10 h each, followed by washing with deionized water and then with a dilute NH_4OH solution (pH = 9.5). Heating of this NH_4−USY in a N_2 flow (or *in vacuo*, for calorimetry and FTIR) at a rate of 2 K/min to 573 K and then maintaining it at 573 K for 16 h produced (H,NH_4)−USY(26). 0.323 mmol/g of NH_3 remained in this sample (24% of the total sites), as determined by temperature programmed desorption of all remaining ammonia. Calcination of (NH_4)−USY in a ceramic dish in open air at 723 K for 10 h produced H−USY(26)-2.

Physical Characterization

The crystallinities and unit cell constants (a_0) of the zeolites were obtained by powder XRD. The number of

TABLE 1

Properties of the Zeolites

Sample	Treatment	a_0 (Å)	XRD Al_F/u.c.	XRD crystallinity	N_2 MPV[a] (cm^3/g)	Na (wt%)	Surface area (m^2/g)
Na−Y	None	24.671	55	105	0.321	10.1	715
NH_4−Y	NH_4^+, exch. Na−Y	24.75	(55)[b]		0.292	0.13	651
H−Y(51)	NH_4−Y, calc. 573 K/16 h	24.633	51	98	0.348	0.13	764
H−USY(26)	NH_4−USY, calc. 723 K/16 h	24.468	26	99	0.252	0.10	550
H−USY(17)	H−USY(26), steam 808 K/1 h	24.386	17	92	0.240	0.10	532
H−USY(8)	H−USY(26), steam 973 K/3 h	24.308	8	78	0.218	0.10	483
(H,NH_4)−USY(26)	NH_4^+, exch. H−USY(26), calc. 573 K/16 h		(26)[c]		0.282		618
H−USY(26)-2	NH_4^+, exch. H−USY(26), calc. 723 K/10 h		(26)[c]				

[a] Micropore volume.

[b] The Al_F content of NH_4−Y was assumed to be equal to that of Na−Y (see Experimental section).

[c] Al_F content was estimated from the Al_F content of the parent sample, H−USY(26).

framework Al atoms per unit cell (Al_F/u.c.) for Na–Y and H–Y was obtained using the correlation

$$Al_F/\text{u.c.} = 115.2(a_0 - 24.191), \quad [1]$$

which was derived (33) for Na–X and Na–Y zeolites. This correlation is not appropriate for NH_4–Y since ammonium cations cause a lattice expansion of the unit cell. For dealuminated zeolites, the Al_F contents were calculated from Eq. (2),

$$Al_F/\text{u.c.} = 112.4(a_0 - 24.233) \quad [2]$$

which is suitable for steam dealuminated zeolites (34). The XRD crystallinity, Al_F/u.c., N_2 micropore volume, and surface area data are summarized in Table 1. They all show that the zeolites were highly crystalline, although H–USY(8) had a somewhat lower crystallinity than the other zeolites.

The three H–USY and the NH_4–Y samples were analyzed by ^{27}Al MAS-NMR. The NMR spectra are shown in Fig. 1. They were collected using a spinning rate of 14 kHz, a 90° (1 A · s) excitation pulse, and a 5 ps time between pulse and acquisition. From the areas of the 60 ppm peak relative to the other peaks, and assuming that the samples all contained a total of 55 Al atoms per unit cell, the tetrahedral Al contents of H–USY(26), H–USY(17), and H–USY(8) were calculated to be 28, 26, and 21 Al/u.c., respectively. In the H–USY samples, the width of the tetrahedral (60 ppm) resonance was much larger than that usually observed for framework species (NH_4–Y). This was due in a large part to the presence of nonframework tetrahedral Al species. Therefore, the XRD values were used instead of the NMR results to estimate the Al_F contents.

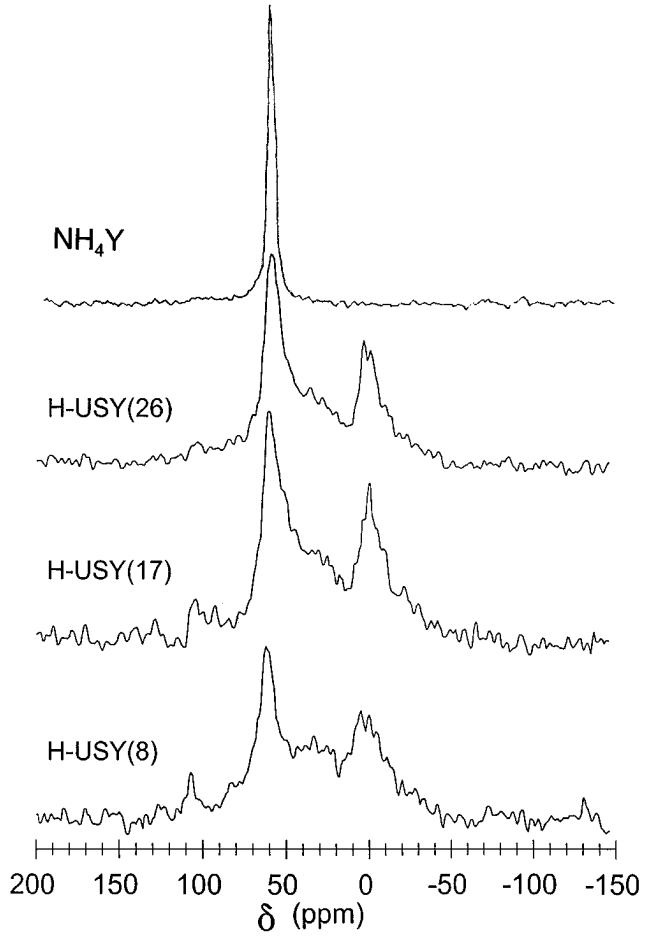

FIG. 1. ^{27}Al MAS NMR spectra of the H–USY and NH_4–Y samples.

Acidity Measurements

The number of acid sites in each zeolite was determined by ammonia TPD, using standard procedures (35–37) but with the following modification. The zeolites were exchanged with 10% ammonium nitrate solution, thoroughly washed (3 × 50 ml at 353 K for 5 g zeolite) to remove excess ammonium ions, and air-dried at 373 K before NH_3 desorption. This procedure eliminated physisorbed ammonia and retained chemisorbed ammonia.

The acid strength distributions were measured by NH_3 adsorption microcalorimetry. The zeolite was pressed into a large wafer at 39 MPa (5700 psi), then broken into 20/40 mesh pieces. The calorimeter sample cell was loaded with 0.3 g of zeolite pieces, and the reference cell contained an equal volume of 25/45 mesh quartz chips. The samples were pretreated *in vacuo* at 573 K for 16 h, then cooled to 473 K for measurements. Doses of NH_3 were admitted to the sample cell, while the heat evolved for each dose was monitored by means of a Tian–Calvet-type calorimeter. Upon admission of a dose, the pressure in the cell increased initially and then rapidly returned to the value before the dose. The apparent equilibrium pressure after 20 to 80 min increased by a small, constant increment with each dose, possibly resulting from small leaks in the system; nevertheless, the pressure always returned to less than 7 Pa (0.05 Torr) at low NH_3 coverages. At moderate coverages, when the heat of adsorption was 118–122 kJ/mol, the final pressure increased more rapidly with each dose. The pressure rise per dose continued to increase with dosage. When the heat of the NH_3 adsorption was close to 90 kJ/mol, the final pressure was rising at a large, approximately constant rate with increasing coverage. Therefore, all acid sites were assumed to be saturated when the heat of adsorption reached 90 kJ/mol.

The calorimeter sensitivity was originally calibrated using the Joule effect, by measuring the output of the heat flux transducers in response to a measured electric current through a resistor, which was covered with quartz chips in the sample cell. The reproducibility of measurements was periodically checked. Recalibration of the calorimeter was also achieved by repeating NH_3 adsorption measurements on an H-ZSM-5 standard (CBV-5020, Conteka). Because of its homogeneous acid strength distribution,

H-ZSM-5 permitted both the quantity of NH_3 adsorbed and the heat flux sensitivity to be calibrated in a single experiment. Over a coverage range of 0.07 to 0.37 mmol/g, the heat of adsorption was nearly constant at 133–135 kJ/mol, and dropped rapidly from 130 to 90 kJ/mol for coverages of 0.42 to 0.54 mmol/g.

FTIR spectra of adsorbed NH_3 were collected using a Mattson Galaxy 5022 spectrometer. The zeolite powder was pressed at 190 MPa (28,000 psi) to make a wafer weighing approximately 4 mg/cm^2. The wafer was mounted in an IR cell and pretreated *in vacuo* at 573 K for 16 h. The wafer was then cooled to 473 K, and measured doses of NH_3 were admitted to the cell. After the NH_3 dose was allowed to equilibrate with the wafer for 10–20 min, a spectrum was collected.

Adsorption on Brønsted acid sites was detected by the appearance of a peak at 1440 cm^{-1}, and on Lewis sites by peaks at 1310 and 1624 cm^{-1} (38). The increases in the areas of the 1624 and 1440 cm^{-1} peaks for each NH_3 dose were obtained by fitting Gaussian curves to the differences of the two spectra, taken before and after the dose. The molar integrated absorption coefficient for the 1440 cm^{-1} peak was estimated to be 12 ± 4 cm/μmol from spectra of NH_3 on H−Y(51), which contained mostly Brønsted sites. For the 1624 cm^{-1} band, the absorption coefficient was estimated by NH_3 adsorption on γ-Al_2O_3 (Johnson Matthey, 99.97% purity) to be 1.0 ± 0.4 cm/μmol. Thus, the absorption coefficient for the 1440 cm^{-1} band was roughly 12 ± 6 times larger than that of the 1624 cm^{-1} band. Because the 1310 and 1624 cm^{-1} bands always increased at approximately equal rates with increasing coverage, the band at 1624 cm^{-1} was used to calculate the amounts adsorbed on all Lewis acid sites which interacted with NH_3.

2-Methylpentane Cracking Activity

Cracking of 2-methylpentane was carried out in a tubular, 7.4 mm i.d., flow microreactor at 573 K. At this temperature, 60–90% of the reaction products were isomers of 2-methylpentane (mainly 3-methylpentane), and the fraction of product which was isomerization products decreased with increasing conversion for all of the catalysts. These isomerization products were not included in the calculation of cracking activity. Thus, cracking conversion was defined as the conversion to C_1–C_8 products, excluding hexane isomers, and the percent selectivity of a product was the percent based on all cracked products excluding C_6 isomers.

Each zeolite was pressed into a large wafer at 39 MPa (5700 psi), then broken into 50/80 mesh pieces. 0.02 to 0.5 g of zeolite was mixed with an amount of 30/50 mesh α-Al_2O_3 chips (Atlantic Equipment Engineers, 99.9% purity) sufficient to make a total bed volume of 1.4 cm^3 in the flow reactor. An additional 0.5 cm^3 of α-Al_2O_3 was added to the top of the catalyst bed to preheat the feed gases. Except for H−Y and (H,NH_4)−USY, all the catalysts were pretreated by heating in N_2 flow at 10 K/min to 573 K and holding at 573 K for 0.5–1 h. H−Y and (H,NH_4)−USY were prepared *in situ* from the ammonium forms by heating in a N_2 flow at 2 K/min to 573 K and holding it for 16 h at 573 K. The cracking activity of (H,NH_4)−USY was also tested after pretreatment in vacuum instead of N_2 flow, to evaluate the effect of the different pretreatment used for FTIR and calorimetry.

Nitrogen was saturated with 2-methylpentane (Aldrich, 99+% purity) at 273 K and passed through the reactor, giving a 2-methylpentane molar feed flow rate of 4.4–8.7 mmol/h. Reaction products were analyzed by an online gas chromatograph with a flame ionization detector (FID), and the weight percentage selectivities were calculated assuming an FID response factor of 1.0 for all hydrocarbons (39). For some of the catalytic runs, products were separated by a 10 ft. 1/8 in. stainless steel column packed with 80/100 mesh *n*-octane/Porasil C (Alltech), using a temperature program: heating for 5 min at 353 K, and then at a rate of 20 K/min from 353 to 418 K. Additional runs were performed using a 5% phenyl, methylsiloxane capillary column to separate products (Hewlett Packard, 30×0.32 mm, with 0.25 μm film thickness), at 303 K, with a split ratio of 50 and a column flow rate of 2.6 cm^3/min. The cracking conversion was measured at several values of time on stream (typically at 2, 22, 42, and 62 min for the packed column, and at 1, 6, 11, 16, 21, 30, 40, 50, 80, and 110 min for the capillary column). The initial conversion was determined by extrapolating to zero time using an empirical equation, Eq. [3],

$$X = X_0 \exp\left(-k_d t^{0.4}\right), \qquad [3]$$

where X is the fractional conversion at time t, X_0 is the conversion at zero time, k_d is the deactivation rate constant, and t is the time on stream. The exponent of 0.4 allowed a better fit to the data than 0.5, the value used previously (40).

By varying the catalyst weight, various initial cracking conversions (X_0) were obtained for each sample, ranging from 2 to 30%. Assuming first-order kinetics, $-\ln(1 - X_0)$ was plotted against the catalyst weight divided by the 2-methylpentane flow rate (W/F) to obtain a linear plot, the slope of which was a rate constant per unit weight of catalyst. In the absence of zeolite, there was no measurable conversion of 2-methylpentane at 573 K over α-Al_2O_3.

RESULTS

Thermal Stability of H−Y

H−Y zeolite, prepared by heating of NH_4−Y, was thermally unstable with respect to further heating. The N_2 micropore volume and surface area of H−Y(51) after being heated under vacuum to 523 K at 1 K/min followed by 16 h at 523 K was 0.05 cm^3/g and 110 m^2/g (compared to 0.35 cm^3/g and 715 m^2/g for Na−Y), indicating that the crystallinity was

about 15%. In addition, the XRD unit cell size was 24.60 Å, suggesting that there was little dealumination in the crystalline portion. Even drying at 373 K resulted in the loss of zeolite crystallinity: the micropore volume and surface area were 0.1 cm^3/g and 220 m^2/g, corresponding to about 30% crystallinity. However, the crystallinity of NH_4–Y calcined overnight at 2 K/min to 573 K in flowing N_2 was nearly 100%, with no dealumination. Although TPD analysis showed that 8% of the NH_4^+ ions remained adsorbed on the acid sites, a pretreatment temperature of 573 K was chosen because this was the maximum temperature allowed by the calorimeter system. Therefore, the standard preparation method of H–Y(51) which resulted in high crystallinity and no dealumination was heating of NH_4–Y(51) in flowing N_2 (or *in vacuo*, for calorimetry and FTIR) at 2 K/min to 573 K, followed by 16 h at 573 K.

Microcalorimetry of NH_3 Adsorption on H–Y and H–USY

Figure 2 shows the differential heat of NH_3 adsorption on H–Y(51) and H–USY(26) at 473 K. H–Y(51) had a total acid site concentration (sites with heats >90 kJ/mol) of 4.4 mmol/g, but only 3% (0.12 mmol/g) of the acid sites adsorbed NH_3 with a heat of adsorption >125 kJ/mol. The heat for the strongest acid sites was about 130 kJ/mol. Approximately 2.0 mmol/g of sites adsorbed NH_3 with a rather constant heat of 121–123 kJ/mol, indicating a generally homogeneous acid strength distribution. At coverages above about 2.5 mmol/g, the differential heat of adsorption decreased with increasing coverage. These results are consistent with the literature. Unsteamed H–Y zeolites, with Na at 10–25% of the exchange sites, have a rather homogeneous acid strength, and the reported heat of NH_3 adsorption is generally near 110–120 kJ/mol (10, 38, 41–46).

In H–USY(26), the total acid site concentration was 1.37 mmol/g, and half of the acid sites (0.68 mmol/g) had heats of NH_3 adsorption >125 kJ/mol. The heat for the strongest acid sites was about 150 kJ/mol. In contrast to H–Y(51), the acid strength distribution in H–USY(26) was heterogeneous and decreased with increasing NH_3 surface coverage. Thus, there were over twice as many acid sites in H–Y(51) as in H–USY(26), but the latter contained a larger number of stronger acid sites. In agreement with these results, the literature reports a heterogeneous acid strength distribution for H–USY. The heat of NH_3 adsorption on the strongest acid sites is generally reported to be between 130 and 175 kJ/mol (10, 40, 44, 47–49), although this value probably depends on the steaming and pretreatment conditions.

The differential heats of NH_3 adsorption on H–USY(26), H–USY(17), and H–USY(8) are compared in Fig. 3. With increasing severity of steaming, there was a decrease in the total number of acid sites, consistent with the decrease

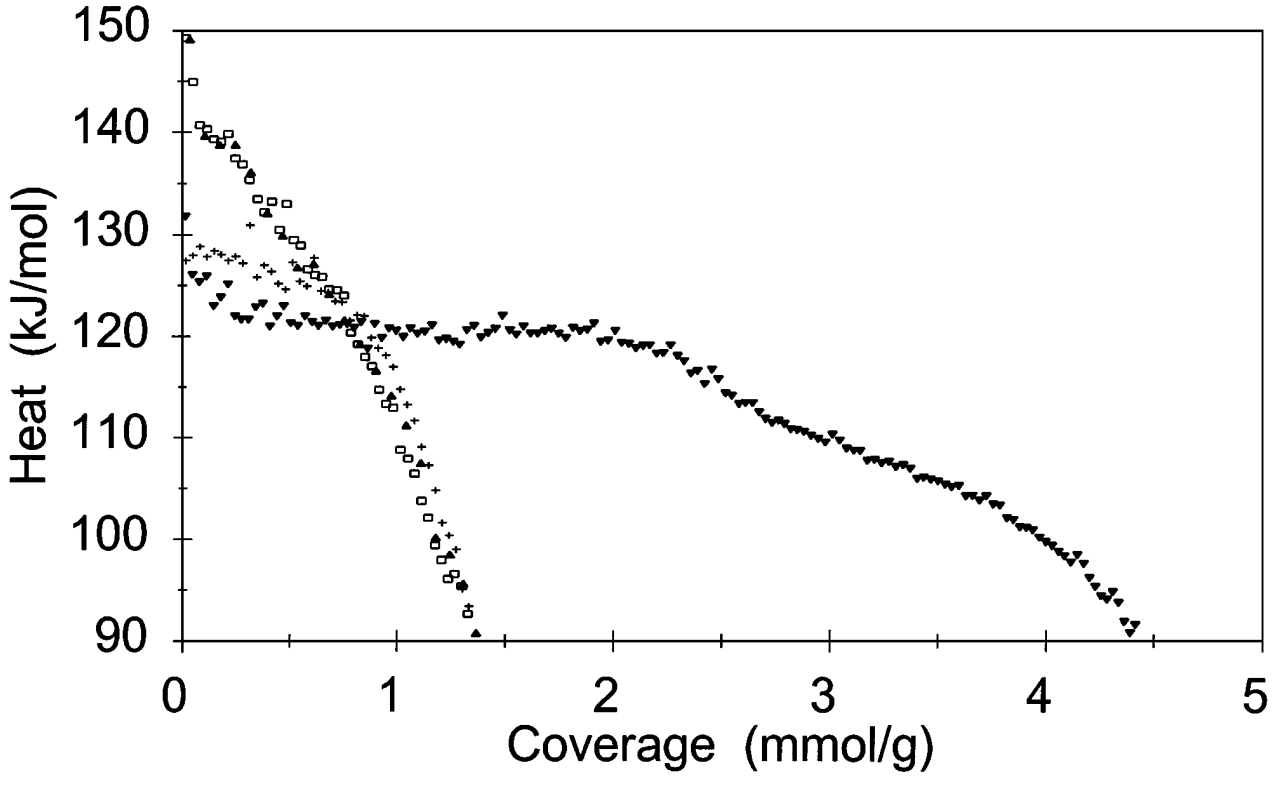

FIG. 2. Differential heat of NH_3 adsorption at 473 K on (▼) H–Y(51), (+) (H,NH_4)–USY(26), (▲) H–USY(26)-2, and (□) H–USY(26).

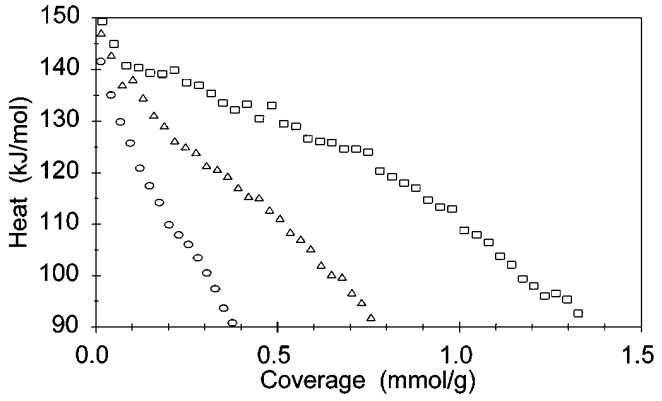

FIG. 3. Differential heat of NH_3 adsorption at 473 K on (□) H−USY(26), (△) H−USY(17), and (○) H−USY(8).

in the Al_F/unit cell determined by XRD. In H−USY(17) the total number of acid sites was 0.79 mmol/g, and for H−USY(8) 0.39 mmol/g. Although the initial heat of adsorption was relatively unchanged at about 145 ± 5 kJ/mol, additional steaming caused a proportionally greater loss in sites with heats near 130–140 kJ/mol than in weaker sites (Fig. 4). Whereas 36% of the sites in H−USY(26) had heats $\geq$130 kJ/mol, only 22% of the sites in H−USY(17), and 17% in H−USY(8) had such high heats.

Table 2 compares the number of acid sites determined by NH_3 TPD and microcalorimetry with the Al_F concentration, determined by XRD. The Al_F concentration, in mmol/g, was calculated according to Eq. [4],

$$Al_F \text{ conc.} = (\%\text{crystallinity}/100)\ (Al_F/\text{u.c.})/(11.520\ \text{g/mmol}), \quad [4]$$

where the crystallinity and the Al_F/u.c. were determined from XRD (Table 1), and 11.520 g was the weight of

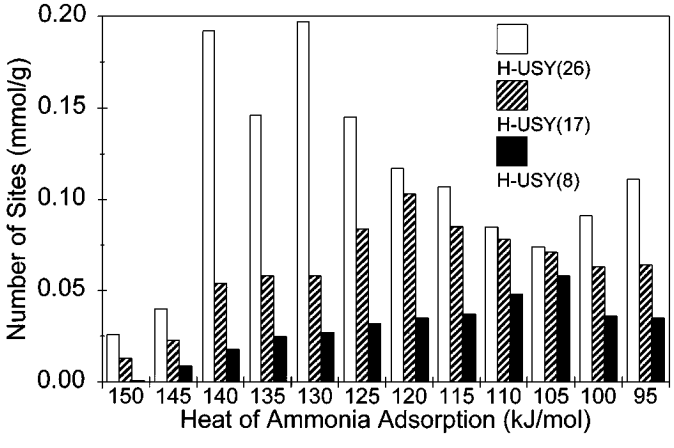

FIG. 4. Distribution of NH_3 adsorption heats for the three H−USY catalysts. Each bar represents the number of acid sites with the given heat value ±2.5 kJ/mol.

TABLE 2

Comparison of Framework Al Content, Acid Site Concentration, and Cracking Rate Constants

Sample	Al_F XRD (mmol/g)	Acid sites TPD (mmol/g)	Acid sites Calorimetry[a] (mmol/g)	k_g (±20%) (μmol/g-s)
H−Y(51)	4.3	4.0	4.4	0.3
H−USY(26)	2.3	1.6	1.37	10
H−USY(17)	1.4	0.93	0.79	4
H−USY(8)	0.57	0.30	0.39	0.8
(H,NH_4)−USY(26)			1.37	10
H−USY(26)-2			1.38	13

[a] Number of acid sites with heat of NH_3 adsorption >90 kJ/mol.

one mmol unit cells. For the total number of acid sites from microcalorimetry, all sites with adsorption heats of >90 kJ/mol were counted. Previous microcalorimetric studies have chosen 80 kJ/mol (10, 41, 44, 50, 51) or 90 kJ/mol (40, 52) as the lower limit for chemisorption of NH_3 on acid sites. For all of the catalysts, Table 2 shows very good agreement between the number of sites with heats >90 kJ/mol and the acid site concentration by TPD. For H−Y(51), there was very good agreement between the Al_F concentration and the total number of acid sites from calorimetry and TPD. However, the acid site concentrations in the three H−USY catalysts were only approximately half of the Al_F concentration. This has been observed previously in H−USY and steamed zeolites (48–54). It appears that some of the Al_F atoms are charge compensated by Al_{NF} cations, rather than by acidic protons.

FTIR of NH_3 Adsorption

NH_3 adsorption was performed in an *in situ* FTIR cell to determine the type of acid sites present. Wafers of the zeolites were pretreated for 16 h at 573 K, and spectra of the fresh zeolites were obtained at 473 K. Additional spectra were collected after adsorption of measured NH_3 doses. Figure 5 shows the difference spectra of NH_3 adsorbed on H−Y(51). Adsorption on Brønsted acid sites produced an intense peak at 1435 cm^{-1}. Peaks for adsorption on Lewis acid sites (1310 and 1624 cm^{-1}) were not observed.

Figures 6a–6c are difference spectra for three different coverages of NH_3 adsorbed on H−USY(26). At low coverages, there was an intense band at 1440 cm^{-1} for adsorption on Brønsted acid sites and weak bands at 1624 and 1310 cm^{-1} for adsorption on Lewis acid sites. With increasing coverage, the ratio of Lewis/Brønsted adsorption increased. The spectra for H−USY(17) and H−USY(8) were qualitatively similar to those of H−USY(26).

Using the known ratio of the absorption coefficients for the 1440 and 1624 cm^{-1} bands (see the Experimental section), the relative amounts of NH_3 adsorbed on Brønsted

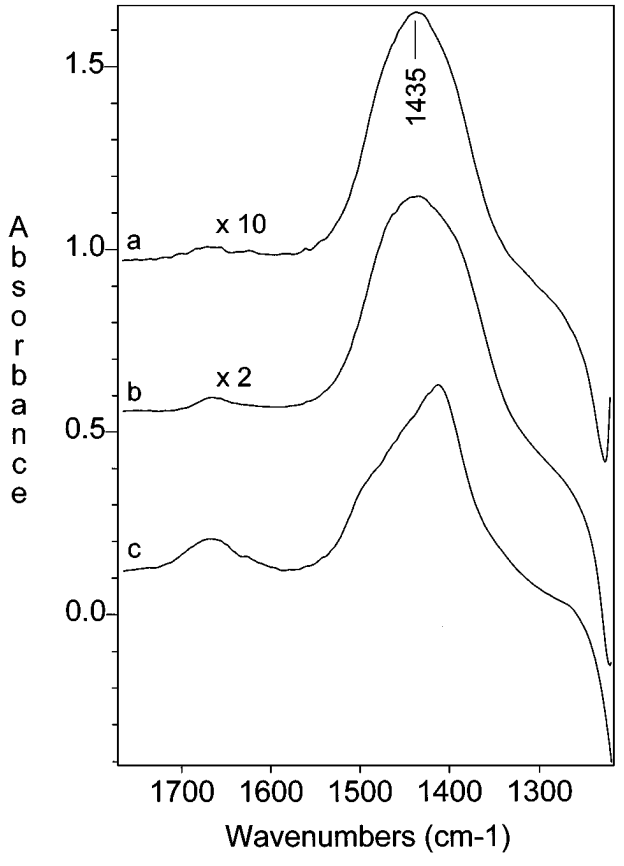

FIG. 5. FTIR difference spectra of NH_3 adsorbed on H−Y(51) at 473 K, showing the difference between spectra taken at coverages of (a) 0.1 and 0 mmol/g; (b) 1.0 and 0.1 mmol/g; and (c) 3.4 and 1.0 mmol/g.

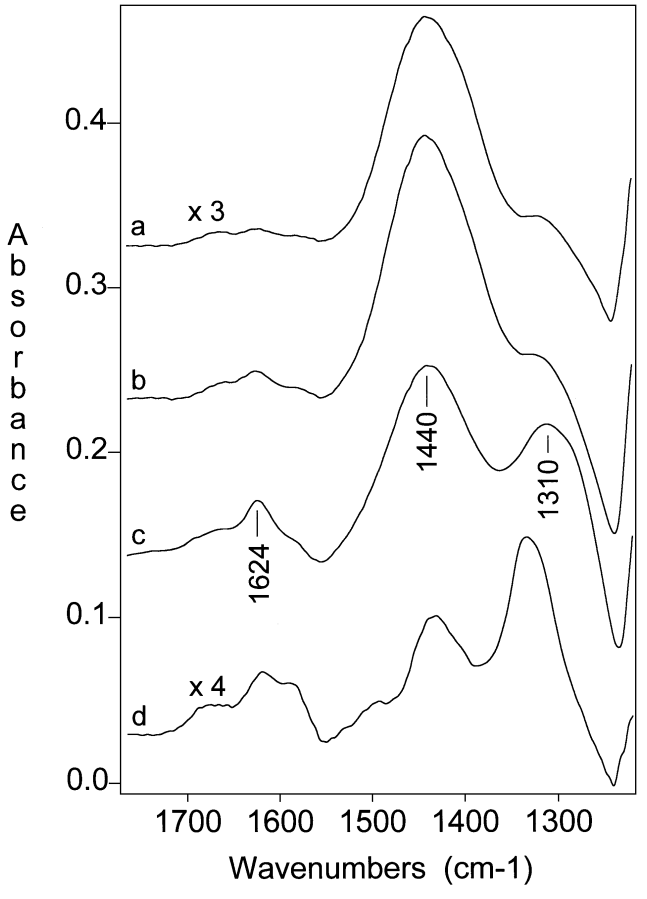

FIG. 6. FTIR difference spectra of NH_3 adsorbed on H−USY(26) at 473 K, showing the difference between spectra taken at coverages of (a) 0.1 and 0 mmol/g; (b) 0.5 and 0.1 mmol/g; and (c) 1.0 and 0.5 mmol/g. Spectrum (d) is for H−USY(26) that was saturated with 1.2 mmol/g NH_3 and then heated under vacuum for 8 h at 573 K (referenced to the spectrum of the sample before adsorption).

and Lewis acid sites could be calculated for each dose. Assuming that all of the NH_3 in a dose was adsorbed on either a Lewis site or a Brønsted site, the fraction of each dose adsorbed on Lewis sites was calculated and plotted in Fig. 7 for the three H−USY catalysts. For H−USY(26) and H−USY(17), at coverages below 0.3 mmol/g, approximately 30% of each NH_3 dose was adsorbed on Lewis acid sites, and the remaining 70% on Brønsted sites. Because of the large uncertainty in the relative FTIR absorption coefficients, the fraction of Lewis sites may be in error by ±0.2. However, the qualitative trend can be stated with certainty. With increasing coverage, a larger percentage of each dose was adsorbed on Lewis acid sites.

2-Methylpentane Cracking of H−Y and H−USY

Figure 8 shows the first-order kinetics plot for cracking of 2-methylpentane at 573 K. Each of the data points represents one catalytic run, and multiple runs were performed for each catalyst, using a fresh catalyst sample for each run. The initial conversion for each run (X_0), which corresponded to the activity of a coke-free sample, was calculated using Eq. [3] (see the Experimental section). The rate

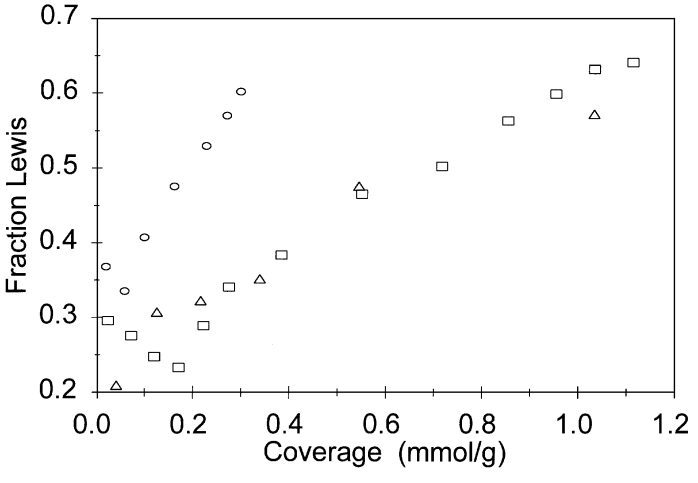

FIG. 7. Fraction of each NH_3 dose adsorbed on Lewis acid sites in (□) H−USY(26), (△) H−USY(17), and (○) H−USY(8).

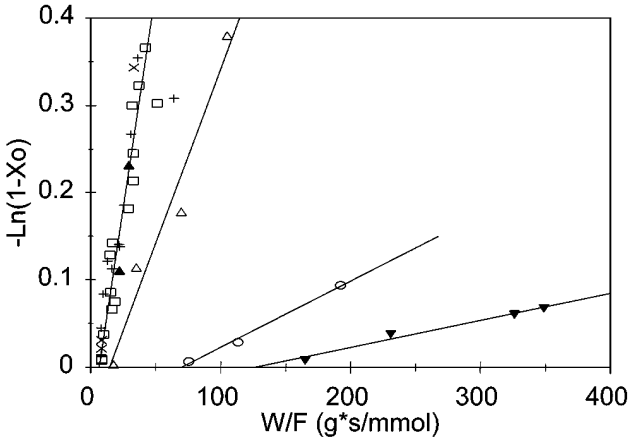

FIG. 8. First order kinetics plot for 2-methylpentane cracking at 573 K, over (□) H−USY(26), (+) (H,NH_4)−USY(26), (△) H−USY(17), (○) H−USY(8), (▼) H−Y(51), (×) H−USY(26)-2, and (▲) (H,NH_4)−USY(26) which was pretreated in vacuum instead of N_2 flow.

constants per unit weight of catalyst, k_g, determined from the slopes of these plots, are shown in Table 2. As previously observed, the k_g for H−USY decreased with increasing severity of steaming, owing to a decrease in the number of acid sites. Thus, the activity per acid site was similar for the three H−USY catalysts. In contrast, the activity per site of H−Y(51) was lower by almost two orders of magnitude. Within experimental uncertainty, the cracking activity was the same for samples pretreated in vacuum and in N_2 flow.

Figure 8 also shows that extrapolation to zero conversion did not pass through the origin. That is, a minimum catalyst weight was required to achieve a measurable cracking conversion. This behavior might result from the initial isomerization of 2-methylpentane to 3-methylpentane or dehydrogenation to form initial olefins, prior to cracking.

All catalysts, including H−Y, H−USY, and (H,NH_4)−USY, had the same distribution of cracking products (C_1−C_8 products, excluding hexane isomers). At 7% cracking conversion, the main products were propane (9%), propene (2%), iso-C_4's (36%), *n*-C_4's (5%), C_5's (34%), and C_7^+ (13%). At all conversions studied, the propene selectivity increased with decreasing conversion. Below 2% conversion, the selectivities to both propane and propene increased sharply, and at 1% conversion they were 15 and 9%, respectively.

Effect of Residual NH_3 on Cracking Activity and Acidity

In order to preserve crystallinity, the H−Y(51) sample was prepared by heating to only 573 K. As a result, 8% of the ammonia remained in the H−Y after pretreatment. The effect of such residual ammonia on the activity of H−USY(26) was examined using the sample (H,NH_4)−USY(26), which was prepared by ion exchange of H−USY to the NH_4^+ form, followed by calcination at 573 K. As shown in Table 2, the activity of (H,NH_4)−USY(26) was equal to that of fresh H−USY(26), suggesting that the 573 K pretreatment was adequate to regenerate a majority of the active sites.

The differential heat of NH_3 adsorption on (H,NH_4)−USY(26) is shown in Fig. 2. Interestingly, unlike H−USY, the acid strength of (H,NH_4)−USY(26) was much more homogeneous, ranging from 125 to 128 kJ/mol, which was 4 to 7 kJ/mol higher than the acid strength of H−Y(51). The total number of acid sites with heat >90 kJ/mol is about the same for (H,NH_4)−USY(26) and H−USY(26), indicating that the lost Lewis sites were replaced by an approximately equal number of Brønsted sites.

FTIR of NH_3 on (H,NH_4)−USY(26) are shown in Fig. 9. For coverages up to about 0.4 mmol/g, adsorption was only on the Brønsted acid sites (1440 cm^{-1} band). Upon increasing the coverage to 1 mmol/g, a small peak at 1626 cm^{-1} appeared, which may be due to Lewis sites, but the peak at 1310 cm^{-1} was not observed. Thus, the residual NH_3 eliminated the strong Lewis acid sites which were present in the H−USY(26) parent sample.

(H,NH_4)−USY(26) was calcined at 723 K for 10 h (like H−USY). This sample, denoted H−USY(26)-2, was characterized by microcalorimetry and FTIR of NH_3 adsorption. Within experimental error, the differential heat of NH_3 adsorption (Fig. 2) was indistinguishable from that of H−USY(26) (55). An FTIR spectrum of NH_3 adsorbed on this sample also shows adsorption on Lewis acid sites

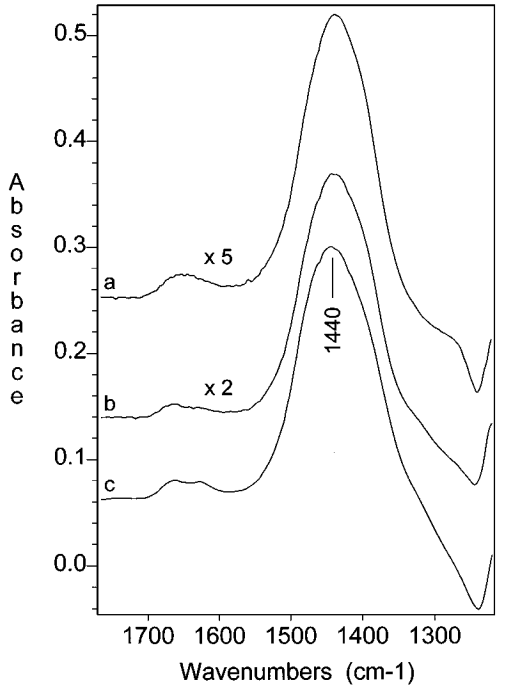

FIG. 9. FTIR difference spectra of NH_3 adsorbed on (H,NH_4)−USY(26) at 473 K, showing the difference between spectra taken at coverages of (a) 0.1 and 0 mmol/g; (b) 0.4 and 0.1 mmol/g; and (c) 1.0 and 0.4 mmol/g.

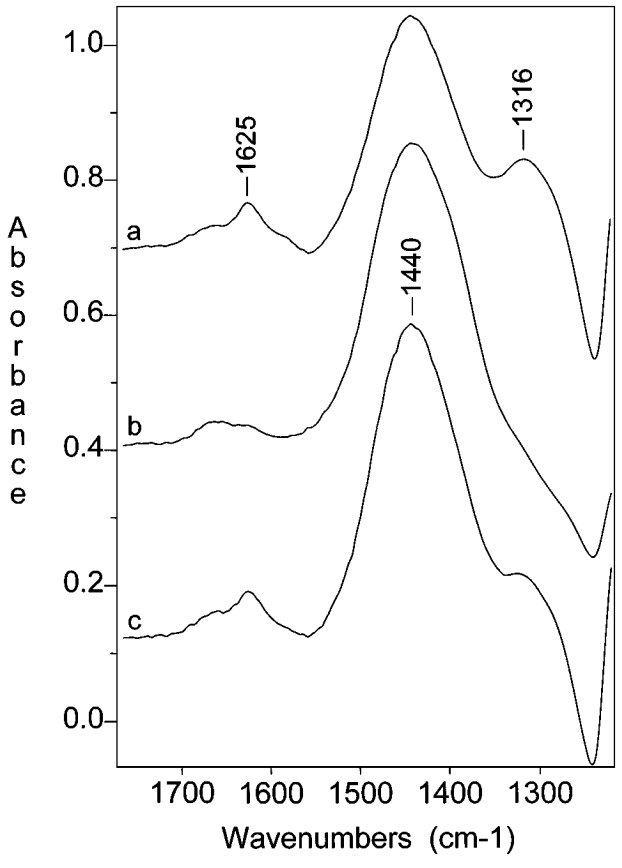

FIG. 10. FTIR spectra of 1.2 mmol/g NH_3 adsorbed at 473 K on (a) H−USY(26), (b) (H,NH_4)−USY(26), and (c) H−USY(26)-2.

(Fig. 10c), which is similar to H−USY(26) (Fig. 10a), but different from (H,NH_4)−USY(26) (Fig. 10b). Furthermore, within experimental error, the cracking activity was similar to that of H−USY(26) also (Table 2). These results show that the sample (H,NH_4)−USY(26) is essentially an H−USY zeolite but with the strong Lewis acid sites covered with NH_3. There was no permanent change in the zeolite as a result of the ion-exchange procedure, because the changes were reversible by desorption of NH_3.

DISCUSSION

Relationship between Acidity and Cracking Activity

In this study, the acid site concentrations, acid strength distributions, and cracking activities of H−USY and H−Y were directly compared. As is well documented by others, the results show that the TOF's for H−USY are two orders of magnitude higher than that of unsteamed H−Y.

The difference in TOF between H−USY and H−Y was not caused by the poor hydrothermal stability of H−Y. Careful pretreatment of NH_4−Y ensured that H−Y had high crystallinity during reaction. This was confirmed by XRD analysis of the sample immediately after reaction, which indicated a crystallinity of 76%. The low Na content also excludes the possibility that the residual Na (or base in general) poisons the active sites, as was suggested by others (3, 17). The H−Y did contain 8% of the ammonia originally present in NH_4−Y, because it was calcined at a relatively low temperature of 573 K in order to maintain crystallinity. Although some studies have shown a severe poisoning effect from small amounts of NH_3, no loss in activity was observed for an H−USY which was NH_4^+ exchanged and pretreated at the same temperature as H−Y. Thus, the residual NH_3 in H−Y is probably not the reason for its low activity. In conclusion, H−Y(51) is highly crystalline and contains a large concentration of Brønsted acid sites, yet its activity is lower than that of H−USY by a factor of 35. This is consistent with Lunsford's data (5).

The higher activity of H−USY than H−Y is most commonly believed to be a result of increased Brønsted acid strength in H−USY (5). This theory is consistent with microcalorimetic data (Fig. 2), which show that most of the sites in H−Y have heats of NH_3 adsorption <125 kJ/mol, whereas H−USY has many sites with heats of 125–150 kJ/mol. Based on these results, we will define "strong" acid sites as those which have heat of NH_3 adsorption >125 kJ/mol.

FTIR shows strong Lewis acid sites in H−USY, whereas the acid sites in H−Y are exclusively Brønsted sites (Figs. 5 and 6). Since some reports in the literature have proposed that Lewis sites play a catalytic role in hydrocarbon transformations (19–23), their potential contribution to the activity of H−USY is discussed. Table 3 shows per-site rate constants (or TOF's) calculated for the H−USY samples, first by considering all strong sites to be active, and second by counting only strong Brønsted sites as active. Assuming that all strong sites are active, the TOF of H−USY(26) is equal to that of (H,NH_4)−USY, although the latter sample has very few strong Lewis sites. Considering only strong Brønsted sites to be active, the TOF is approximately 1.4 (±0.6) times higher for H−USY. Because of large uncertainties in the rate constants k_g and in the estimation of Lewis acid site peak

TABLE 3

Concentration of Strong Acid Sites (both Lewis and Brønsted), Concentration of Strong Brønsted Sites, and the Corresponding per-Site Rate Constants for 2-Methylpentane Cracking

Sample	Strong[a] acid sites		Strong[a] Brønsted sites	
	Site conc. (mmol/g)	$k_{\text{per-site}}$ (s^{-1})	Site conc. (mmol/g)	$k_{\text{per-site}}$ (s^{-1})
(H,NH_4)−USY(26)	0.63	16 (±3)	0.63	16 (±3)
H−USY(26)	0.68	15 (±3)	0.43	23 (±8)
H−USY(17)	0.24	17 (±3)	0.17	23 (±8)
H−USY(8)	0.10	8 (±2)	0.06	13 (±5)

[a] Having heat of NH_3 adsorption >125 kJ/mol.

areas in the FTIR, it is possible that the TOF for H−USY is very close to, or equal to, that of (H,NH_4)−USY. Previously (40) it was found by pyridine adsorption that approximately 20% of the strong sites in H−USY are Lewis sites (compared to 37% by NH_3 adsorption), giving the result that the TOF for H−USY is only 1.2 times higher. In addition, there is no difference in selectivity or deactivation rate (55) for the catalysts with and without Lewis sites. If Lewis sites were active, one would expect that the cracking mechanism over them would result in a different TOF, product distribution, and deactivation rate than the mechanism over the Brønsted sites. Therefore, we conclude that Lewis sites have little or no cracking activity.

Table 3 also compares the TOF for H−USY steamed to different extents. Within error limits, H−USY(26), H−USY(17), and H−USY(8) had the same TOF, giving additional support to the model that Lewis sites are inactive.

Relationship between Acid Site Type and Heat of Adsorption

For sample (H,NH_4)−USY(26), the heat of adsorption was relatively constant at 125–128 kJ/mol, up to a coverage of 0.6 mmol/g. Similarly, H−Y(51) had a homogeneous acid strength of 121–123 kJ/mol for about 2.0 mmol/g (45%) of its acid sites. Both of these catalysts had very few Lewis sites. In contrast, the acid strength distribution was heterogeneous for H−USY, which had both Lewis and Brønsted sites.

Previous studies have assigned the initial high heats in H−USY to adsorption on Lewis acid sites (8, 48, 56, 57). For example, in a study of USY-based FCC catalysts, IR spectroscopy (57) revealed that sites with heats of pyridine adsorption >180 kJ/mol are predominantly Lewis acid sites. Another study of H−USY showed that the number of Lewis sites measured by CO adsorption matched the number of acid sites with NH_3 adsorption heats >140 kJ/mol (48). In agreement with these studies, Fig. 6a also shows that there are strong Lewis acid sites in H−USY. However, there are many more weak Lewis sites than strong ones, as shown in Fig. 6c, and quantitatively in Fig. 7. The strongest sites, at low NH_3 coverages, are approximately $30 \pm 20\%$ Lewis sites, whereas the weakest sites are $60 \pm 20\%$ Lewis sites.

Although the data do not permit the determination of the acid strength distribution of Lewis sites in H−USY, it is reasonable to suggest that the Lewis sites in H−USY may be heterogeneous. A widely varying heat of adsorption is observed for the Lewis sites in γ-Al_2O_3 (2, 45, 48), which contains very few Brønsted sites (48).

Based on calorimetric data obtained with H−Y, (H,NH_4)−USY, H-ZSM-5 (54, 58), and H-mordenite (45, 54, 58), it appears that adsorption of bases on structural Brønsted acid sites produces a relatively constant heat, suggesting that these sites have a rather homogeneous acid strength. Thus, it is quite possible that a majority of the Brønsted sites in H−USY are also homogeneous. Also, the fact that H−USY and (H,NH_4)−USY had approximately the same TOF suggests that the active sites in the two catalysts are the same. If one assumes that elimination of the Lewis acid sites in (H,NH_4)−USY had no effect on the Brønsted acid sites, then this implies that the Brønsted sites in H−USY also have a uniform NH_3 adsorption heat of 128 kJ/mol. The rapidly decreasing heat of adsorption shown in Fig. 2 could result, if the NH_3 doses did not attain complete equilibrium with the catalyst sample in the calorimeter, so that the heterogeneous Lewis sites were titrated simultaneously with the homogeneous Brønsted sites. To illustrate further, at low NH_3 coverages the heat of adsorption was about 140 kJ/mol, and approximately 30% of each dose was adsorbed on Lewis acid sites. Assuming that the heat of adsorption on the Brønsted sites was 128 kJ/mol, this implies that the heat of adsorption on the Lewis sites was 168 kJ/mol. This is a reasonable value for the heat of NH_3 adsorption on strong Lewis sites (2, 45, 48).

Although it is fairly well accepted that Brønsted sites in zeolites are located on the framework hydroxyl groups, the location and structure of the Lewis sites are less certain. It has been suggested that Lewis sites may be located on nonframework aluminum species similar to alumina (29, 30). However, IR and microcalorimetry show that Al_{NF} species are largely nonacidic. With increased steaming, and formation of additional Al_{NF}, the concentrations of both the Brønsted and Lewis acid sites decreased. Also, Lewis sites were quantitatively converted into Brønsted sites in (H,NH_4)−USY by addition of ammonium ions, suggesting that the Lewis sites may be in the framework.

Extent of Equilibrium in Calorimetry and IR

Measurement of acid strength distributions by NH_3 adsorption microcalorimetry is usually performed at a temperature of at least 423 K (45). Under these conditions, it is generally assumed that the adsorbed NH_3 has sufficient mobility to achieve equilibrium with the acid sites on the catalyst surface in a reasonable amount of time (roughly 1 h or less). Assuming that each NH_3 dose is allowed sufficient time to reach equilibrium, then the initial doses should adsorb on the strongest acid sites, and subsequent doses would titrate successively weaker sites. The decreasing heat of adsorption measured in H−USY suggests at least some degree of equilibration. Otherwise, an apparent homogeneous distribution profile would be obtained. However, the calorimetry by itself does not reveal whether complete equilibration was obtained, particularly on the initial doses that were very strongly adsorbed.

To investigate this further, NH_3 adsorption and desorption IR spectra were compared for a wafer of H−USY(26). After adsorption of NH_3 doses at 473 K to a coverage of 1.2 mmol/g, the IR cell was evacuated and the sample temperature was increased to 573 K. The sample was held at

573 K under dynamic vacuum for 8 h, to allow desorption of any reversibly-adsorbed NH_3, then the wafer was cooled to 473 K and another spectrum collected, Fig. 6d. This spectrum, referenced to the fresh H–USY prior to adsorption, shows peaks for all NH_3 that was irreversibly adsorbed at 573 K. This remaining NH_3 was adsorbed both on Lewis sites (1330 and 1620 cm^{-1}) and Brønsted sites (1432 cm^{-1}). Using the IR absorption coefficients, it was estimated that 0.09 mmol/g of NH_3 was adsorbed on Lewis sites, and only one-third as much (0.03 mmol/g) was adsorbed on Brønsted sites, implying that the strongest sites in H–USY are 75% Lewis sites.

In contrast, adsorption spectra showed that only about 30% of the initial doses were adsorbed on Lewis sites, over the same coverage range of 0–0.12 mmol/g (Fig. 7). In fact, during adsorption of NH_3 doses, the total coverage exceeded 0.30 mmol/g, before the coverage of Lewis sites reached 0.09 mmol/g as observed in the desorption spectrum. These results demonstrate that NH_3 was not equilibrated with the strong Lewis sites at 473 K, and equilibration was probably not attained in the calorimeter at this temperature either.

In light of these results, the microcalorimetric results for H–USY must be interpreted with caution. Although heats in excess of 140 kJ/mol were measured for adsorption at low coverages, this does not imply that the sample necessarily contains Brønsted sites with such a high heat of adsorption, since adsorption occurs on both Brønsted and Lewis sites and equilibration of adsorbed NH_3 among these sites was not achieved. High initial heats were measured because of adsorption on strong Lewis sites, but these sites are catalytically inactive. Thus, when a zeolite contains both Brønsted and strong Lewis acid sites, the heat of adsorption is not a good indication of cracking activity.

In contrast, calorimetry may be useful for comparing zeolites that contain only Brønsted sites, with a fairly homogeneous acid strength. The homogeneous sites in (H,NH_4)–USY(26) had a higher heat of adsorption than those in H–Y(51), and this difference may well be correlated to the activity difference between the two catalysts. However, the difference in the heat of adsorption is small (about 5 kJ/mol). If the heat of NH_3 adsorption is a reasonable measure of the relative Brønsted acid strength, then the observation suggests that the cracking activity must be influenced by factors in addition to acid strength, since in order to account for a 50 times difference in catalytic activities at 573 K, a difference in apparent activation energy of 19 kJ/mol is needed. A possibly important contribution to the high activity of H–USY and (H,NH_4)–USY(26) is the presence of fractures and mesopores formed during steam dealumination (59). These fractures and mesopores would increase the rate of a diffusion-limited reaction by facilitating transport of reactants to the acid sites inside the zeolite particles and the products out. Gas oil cracking activity is enhanced by the presence of mesopores in Y zeolites (60), and there is also evidence to suggest that cracking of smaller molecules such as hexane on H–USY may be diffusion limited (40). It should be emphasized that if the reaction is severely diffusion limited, the formation of mesopores and fractures by steaming only results in much larger observed catalytic activity by increasing the external surface areas for molecules to diffuse into the zeolite channels and micropores, but does not necessarily change the diffusion limitation in the channels and micropores or, consequently, the apparent activation energy.

It is also known in the literature that some of the Brønsted acid sites in H–Y are only accessible to small molecules, such as NH_3, but not to larger molecules, such as pyridine (61, 62). These sites would not participate in the cracking reaction. Steaming of H–Y to form H–USY causes destruction of part of the zeolite structure, exposing some of these sites, making the catalyst more active. While this might also contribute to the enhanced activity in H–USY, because such inaccessible sites represent about 40% of the total Brønsted acid sites in H–Y and there is no evidence that they are stronger acid sites than other Brønsted acid sites, making them accessible for reaction could not account for the 50 times increase in catalytic activity.

In conclusion, the data in this study suggest that strong Lewis acid sites developed during steaming to form H–USY are inactive for hydrocarbon cracking. They can be poisoned with adsorbed NH_3 without significant effect on the cracking activity. The data also imply that Brønsted acid sites in H–USY are homogeneous and stronger compared to H–Y, but this may be by as little as 5 kJ/mol. Therefore, the much enhanced cracking activity in H–USY is due to, at least in part, enhanced mass transport rates because of the presence of fractures and mesopores that are formed by steaming. The results also show that NH_3 adsorption microcalorimetry at 473 K is not completely equilibrated.

ACKNOWLEDGMENTS

Financial support from the National Science Foundation, the Engelhard Corporation, and Ashland Petroleum Company, and in-kind support from Amoco Oil Co., are gratefully acknowledged. The authors also thank Scott Babitz and Alex Chu-Kung for their assistance in performing some of the catalytic runs, and Dr. G. J. Ray of Amoco for obtaining and interpreting the NMR data.

REFERENCES

1. Mirodatos, C., and Barthomeuf, D., *J. Chem. Soc. Chem. Comm.* **39** (1981).
2. Shannon, R. D., Gardner, K. H., Staley, R. H., Bergeret, G., Gallezot, P., and Aroux, A., *J. Phys. Chem.* **89**, 4778 (1985).
3. Fritz, P. O., and Lunsford, J. H., *J. Catal.* **118**, 85 (1989).
4. Shertukde, P. V., Hall, W. K., Dereppe, J., and Marcelin, G., *J. Catal.* **139**, 468 (1993).
5. Lunsford, J. H., *in* "Fluid Catalytic Cracking II" (M. L. Occelli, Ed.), p. 1. American Chemical Society, Washington, D.C., 1991.

6. Makarova, M. A., and Dwyer, J., *J. Phys. Chem.* **97**, 6337 (1993).
7. Makarova, M. A., Al-Ghefaili, K. M., and Dwyer, J., *J. Chem. Soc. Faraday Trans.* **90**, 383 (1994).
8. Aroux, A., and Ben Taarit, Y., *Thermochim. Acta* **122**, 63 (1987).
9. Křivánek, M., Dung, N. T., and Jírů, P., *Thermochim. Acta* **115**, 91 (1987).
10. Lohse, U., Parlitz, B., and Patzelová, V., *J. Phys. Chem.* **93**, 3677 (1989).
11. Dempsey, E., *J. Catal.* **33**, 497 (1974).
12. Dempsey, E., *J. Catal.* **39**, 155 (1975).
13. Mikovsky, R. J., and Marshall, J. F., *J. Catal.* **44**, 170 (1976).
14. Zhidomirov, G. M., and Kazansky, V. B., *Adv. Catal.* **34**, 131 (1986).
15. Beyerlein, R. A., McVicker, G. B., Yacullo, L. N., and Ziemiak, J. J., *in* "Preprints," Vol. 31, p. 190. Division of Petroleum Chemistry, American Chemical Society, Washington, D.C., 1986.
16. Kumar, R., Cheng, W-C., Rajagopalan, K., Peters, A. W., and Basu, P., *J. Catal.* **143**, 594 (1993).
17. Lombardo, E. A., Sill, G. A., and Hall, W. K., *J. Catal.* **119**, 426 (1989).
18. Aboul-Gheit, A. K., *Thermochim. Acta* **191**, 233 (1991).
19. Zholobenko, V. L., Kustov, L. M., Kazansky, V. B., Loeffler, E., Lohse, U., and Oehlmann, G., *Zeolites* **11**, 132 (1991).
20. Corma, A., Planelles, J., Sánchez-Marín, J., and Tomás, F., *J. Catal.* **93**, 30 (1985).
21. Chen, F. R., and Xiexian Guo, *J. Chem. Soc. Faraday Trans.* **88**, 511 (1992).
22. Abbot, J., *Appl. Catal. A* **85**, 173 (1992).
23. Hong, Y., Gruver, V., and Fripiat, J. J., *J. Catal.* **150**, 421 (1994).
24. Jolly, S., Saussey, J., and Lavelley, J. C., *J. Mol. Catal.* **86**, 401 (1994).
25. Beyerlein, R. A., McVicker, G. B., Yacullo, L. N., and Ziemiak, J. J., *J. Phys. Chem.* **92**, 1967 (1988).
26. Lónyi, F., and Lunsford, J. H., *J. Catal.* **136**, 566 (1992).
27. Corma, A., Fornés, V., Mocholí, F. A., Montón, J. B., and Rey, F., *in* "Fluid Catalytic Cracking II" (M. L. Occelli, Ed.), p. 12. American Chemical Society, Washington, D.C., 1991.
28. Bamwenda, G. R., Zhao, Y. X., Groten, W. A., and Wojciechowski, B. W., *J. Catal.* **157**, 209 (1995).
29. Coster, D., Blumenfeld, A. L., and Fripiat, J. J., *J. Phys. Chem.* **98**, 6201 (1994).
30. Gruver, V., and Fripiat, J. J., *J. Phys. Chem.* **98**, 8549 (1994).
31. Garralón, G., Corma, A., and Fornés, V., *Zeolites* **9**, 84 (1989).
32. Haag, W. O., Lago, R. M., and Weisz, P. B., *Nature* **309**, 589 (1984).
33. Breck, D. W., and Flanigen, E. M., *in* "Molecular Sieves," p. 47. Society of Chemical Industry, London, 1968.
34. Fichtner-Schmittler, H., Lohse, U., Engelhardt, G., and Patzelová, V., *Crystal Res. Tech.* **19**, K1 (1984).
35. Karge, H., and Dondur, V., *J. Phys. Chem.* **94**, 765 (1990).
36. Corma, A., Fornes, A., Melo, F., and Herraro, J., *Zeolites* **7**, 559 (1987).
37. Hashiguchi, T., and Sakai, S., *in* "New Solid Acids and Bases: Their Catalytic Properties" (K. Tanabe, H. Hattori, T. Yamaguchi, and T. Tanaka, Eds.), p. 191. Kodansha, Tokyo, 1989.
38. Kosslick, H., Berndt, H., Lanh, H. D., Martin, A., Miessner, H., Anh Tuan, V., and Jänchen, J., *J. Chem. Soc. Faraday Trans.* **90**, 2837 (1994).
39. Dietz, W. A., *J. Gas Chromat.* **5**, 68 (1967).
40. Hopkins, P. D., Miller, J. T., Meyers, B. L., Ray, G. J., Roginski, R. T., Kuehne, M. A., and Kung, H. H., *Appl. Catal. A* **136**, 29 (1996).
41. Aroux, A., Bolis, V., Wierzchowski, P., Gravelle, P. C., and Vedrine, J. C., *J. Chem. Soc. Faraday Trans. I* **75**, 2544 (1979).
42. Mitani, Y., Tsutsumi, K., and Takahashi, H., *Bull. Chem. Soc. Jpn.* **56**, 1921 (1983).
43. Kapustin, G. I., Kustov, L. M., Glonti, G. O., Brueva, T. R., Borovkov, V. Y., Klyachko, A. L., Rubinshtein, A. M., and Kazanskii, V. B., *Kinet. Katal.* **25**, 1129 (1984).
44. Stach, H., Wendt, R., Lohse, U., Jänchen, J., and Spindler, H., *Catal. Today* **3**, 431 (1988).
45. Spiewak, B. E., Handy, B. E., Sharma, S. B., and Dumesic, J. A., *Catal. Lett.* **23**, 207 (1994).
46. Aroux, A., and Vedrine, J. C., *in* "Catalysis by Acids and Bases" (B. Imelik, C. Naccache, G. Coudurier, Y. Ben Taarit, and J. C. Vedrine, Eds.), p. 311. Elsevier, Amsterdam, 1985.
47. Maugé F., Aroux, A., Courcelle, J. C., Engelhard, P., Gallezot, P., and Grosmangin, J., *in* "Catalysis by Acids and Bases" (B. Imelik, C. Naccache, G. Coudurier, Y. Ben Taarit, and J. C. Vedrine, Eds.), p. 91. Elsevier, Amsterdam, 1985.
48. Aroux, A., Muscas, M., Coster, D. J., and Fripiat, J. J., *Catal. Lett.* **28**, 179 (1994).
49. Yaluris, G., Rekoske, J. E., Aparicio, L. M., Madon, R. J., and Dumesic, J. A., *J. Catal.* **153**, 65 (1995).
50. Klyachko, A. L., Kapustin, G. I., Brueva, T. R., and Rubinstein, A. M., *Zeolites* **7**, 119 (1987).
51. Stach, H., Jänchen, J., and Lohse, U., *Catal. Lett.* **13**, 389 (1992).
52. Kapustin, G. I., Brueva, T. R., Kutateladze, G. M., and Klyachko, A. P., *Kinet. Katal.* **28**, 759 (1987).
53. Biaglow, A. I., Parrillo, D. J., Kokotailo, G. T., and Gorte, R. J., *J. Catal.* **148**, 213 (1994).
54. Parillo, D. J., and Gorte, R. J., *J. Phys. Chem.* **97**, 8786 (1993).
55. Babitz, S. M., Kuehne, M. A., Kung, H. H., and Miller, J. T., *Ind. Eng. Chem. Res.* (1997), in press.
56. Shi, Z. C., Aroux, A., and Ben Taarit, J., *Can. J. Chem.* **66**, 1013 (1988).
57. Chen, D., Sharma, S., Cardona-Martinez, N., Dumesic, J. A., Bell, V. A., Hodge, G. D., and Madon, R. J., *J. Catal.* **136**, 392 (1992).
58. Chen, D. T., Sharma, S. B., Filimonov, I., and Dumesic, J. A., *Catal. Lett.* **12**, 201 (1992).
59. Beyerlein, R. A., Choi-Feng, C., Hall, J. B., Huggins, B. J., and Ray, G. J., *in* "Fluid Catalytic Cracking III" (M. L. Occelli and P. O'Connor, Eds.), p. 81. American Chemical Society, Washington, D.C., 1994.
60. Dai, P. E., Neff, L. D., and Edwards, J. C., *in* "Fluid Catalytic Cracking III" (M. L. Occelli and P. O'Connor, Eds.), p. 63. American Chemical Society, Washington, D.C., 1994.
61. Mitani, Y., Tsutsumi, K., and Takahashi, H., *Bull. Chem. Soc. Japan* **56**, 1921 (1983).
62. Corma, A., Fornés, V., Perez-Pariente, J., Sastre, E., Martens, J. A., and Jacobs, P. A., "ACS Symposium Series" (W. H. Frank and T. E. Whyte, Jr., Eds.), Vol. 368, p. 555. American Chemical Society, Washington, D.C., 1988.